

Development of a fluorogenic coupled assay for high-throughput quantitative measurement of terpene synthase kinetics

STUDENT: Arseniy Shumilin

SUPERVISOR: Dr Craig Markin; Manchester Institute of Biotechnology, University of Manchester, UK

Word Count (excl. figure legends, references, and acknowledgements) = 1,034

Introduction and Aims

Terpene synthases (TSs) are enzymes responsible for synthesis of over a third of known natural products, with many having commercial importance. However, currently it is not possible to sustainably produce many of these compounds – for example, as part of a circular low-carbon bioeconomy. An approach to tackle this challenge is to discover more catalytically active enzymes to efficiently produce terpenes. However, current TS screening relies on manual product profile analysis by techniques like GC-MS, not feasible for more than a handful of variants. Here, we describe the development of a real-time fluorogenic assay that will form the basis for a future high-throughput assay using the HT-MEK technology (1, 2).

Terpenes are built from precursors (Fig.1) via the mevalonate (MVA) and the methylerythritol phosphate (MEP) pathways which produce geranyl pyrophosphate (GPP). Subsequent steps produce terpenes of increased molecular complexity. The production of terpenes from GPP is driven by release of pyrophosphate which forms the basis of our assay (Fig. 2).

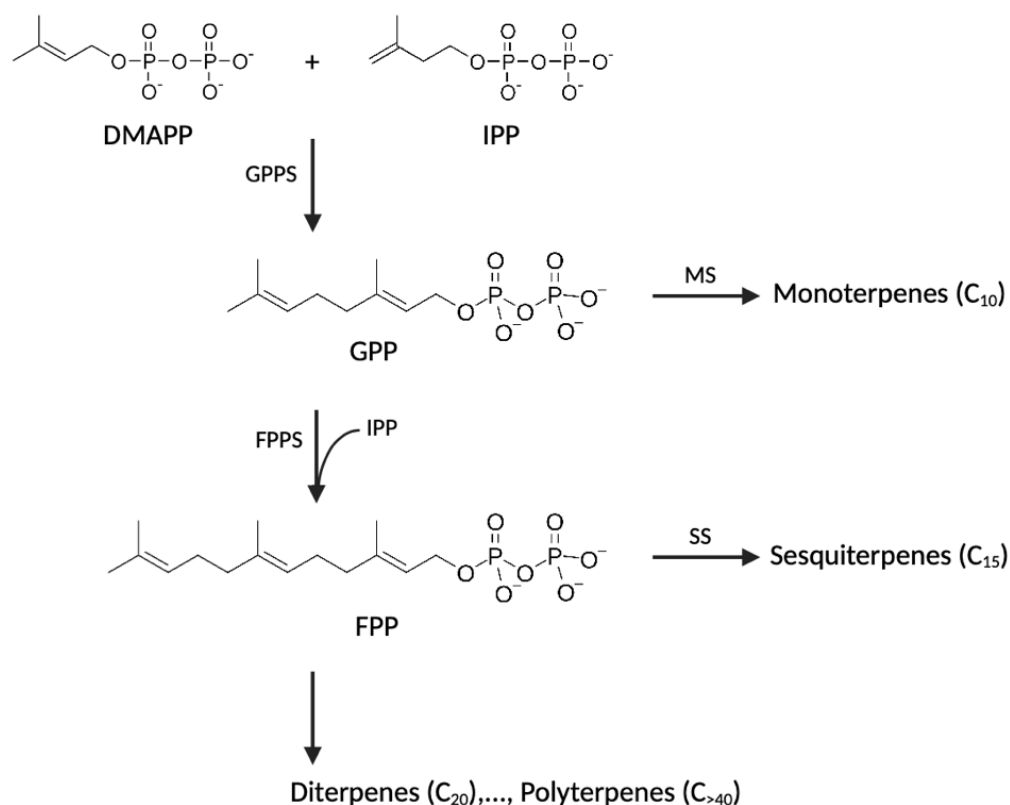


Figure 1. Biosynthetic pathway of terpenes. The pathway begins with the condensation of dimethylallyl pyrophosphate (DMAPP) and isopentenyl pyrophosphate (IPP) to form GPP, which serves as the precursor for monoterpenoids (C₁₀) via monoterpene synthases. Addition of another IPP unit to GPP leads to the formation of farnesyl pyrophosphate (FPP), which allows the formation of sesquiterpenes (C₁₅). Continuous condensations with additional IPP units generate larger precursors, and subsequent classes of terpenes.

Fluorescent detection is enabled by the “Phosphate Sensor” (PS) (3). To couple TS activity to P_i production, we use pyrophosphatase (PPase) to generate P_i which is then detected by the PS (Fig. 2). Our chief aim was therefore to successfully couple the PPase to the TS reaction and ensure TS kinetics could be measured accurately using fluorescence as a detection method.

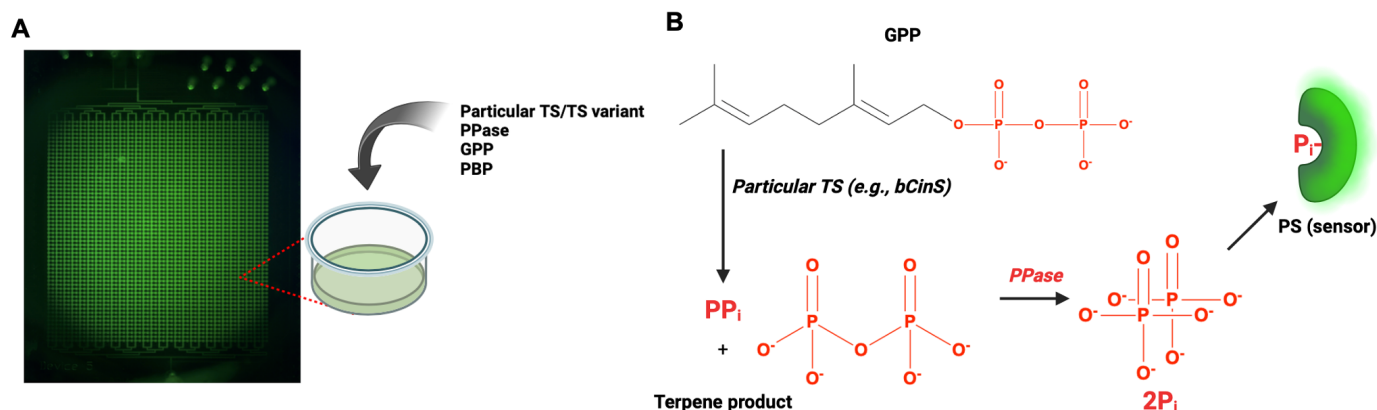


Figure 2. Schematic of coupled assay to measure TS kinetics. (A) HT-MEK microfluidic “chip”, imaged with the bespoke fluorescence imager (see also Fig. 8). (B) Schematic of the fluorogenic coupled assay for measuring TS activity through PP_i release and subsequent detection by PS. PS is *E. coli* phosphate (P_i) binding protein which has a fluorescent molecule covalently linked near its P_i binding site which “turns on” when P_i binds.

Materials and Methods

Standards were prepared using monoanionic and dianionic forms of P_i using the Henderson-Hasselbach equation. The PS was purchased from ThermoFisher Scientific. All reactions were performed at pH 7.6 and run in 384-well microplates in a BMG Labtech CLARIOstar microplate reader and kinetic analyses were performed using Mathematica scripts (1). Levels of P_i contamination were measured in each experiment. Recombinantly expressed bCinS was obtained from Dr Joshua Whitehead. Cell-free expression of bCinS was carried out using PURExpress (NEB). Enzyme concentrations of cell-free expressed bCinS were determined from eGFP fluorescence (1) and P_i was removed via a spin concentrator.

Results

Quantifying absolute $[P_i]$ via fluorescence

We measured a standard curve relating fluorescence of the PS to $[P_i]$. Fluorescence was linear to 50 μM $[P_i]$, allowing us to accurately quantify $[P_i]$ (Fig. 3).

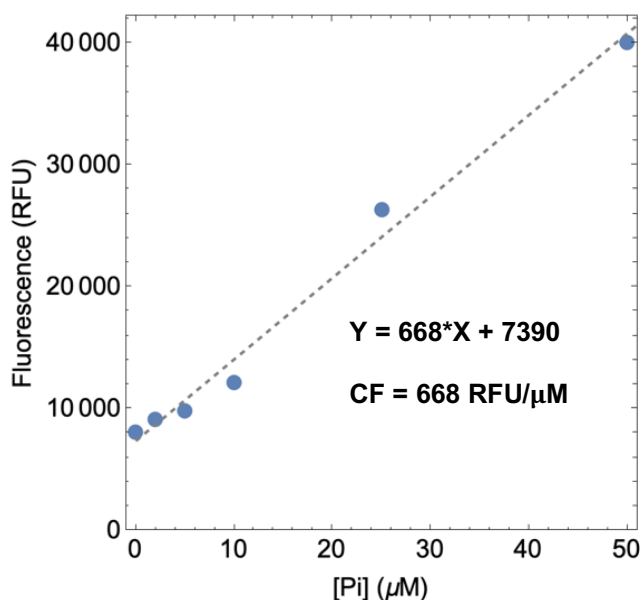


Figure 3. Standard curve relating PS fluorescence to added $[P_i]$. Each additional micromole of P_i corresponds to a 668.0 increase in relative fluorescence units (RFU).

Quantifying kinetics of the PPase step

It is important to measure the PPase activity to ensure that this is not rate-limiting – that the rate of Pi production reflects the rate of GPP hydrolysis by TS. We measured initial rates of PPase hydrolysis at [PPi] concentrations from 0 μM to 100 μM and fit these to the Michaelis-Menten model (Fig. 4).

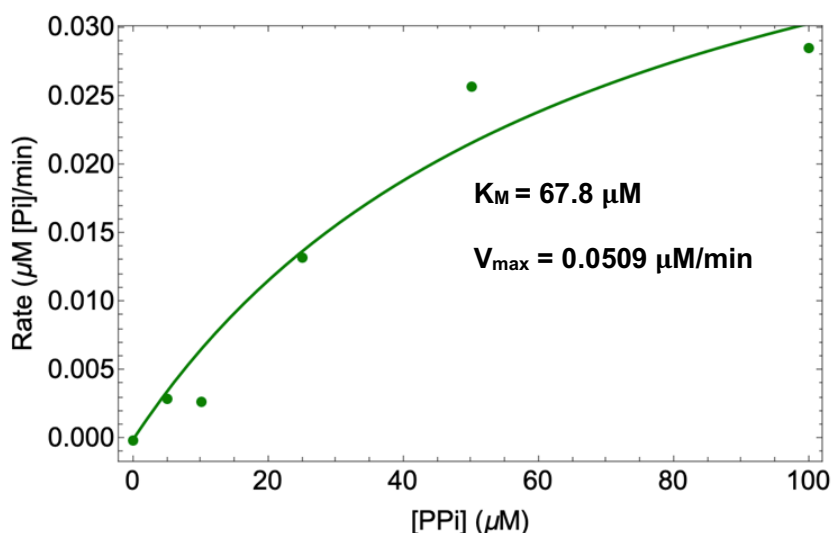


Figure 4. Initial rate measurements of PPase hydrolysis and fit to the Michaelis-Menten model. The PPase is diluted x50,000 from the stock concentration of 0.1 U/ μL .

Measuring background GPP hydrolysis

A piece of information needed to optimise the assay is the spontaneous rate of GPP hydrolysis, as this sets the lower limit of TS detection. We used the PS assay to quantify the spontaneous rate of PP_i release at GPP concentrations spanning 10 μM to 100 μM (Fig. 5a).

Spontaneous rates were low; however, the expected linear relationship was not observed (Fig. 5a). These measurements also allowed us to calculate minimum k_{cat} values measurable using HT-MEK (Fig. 5b).

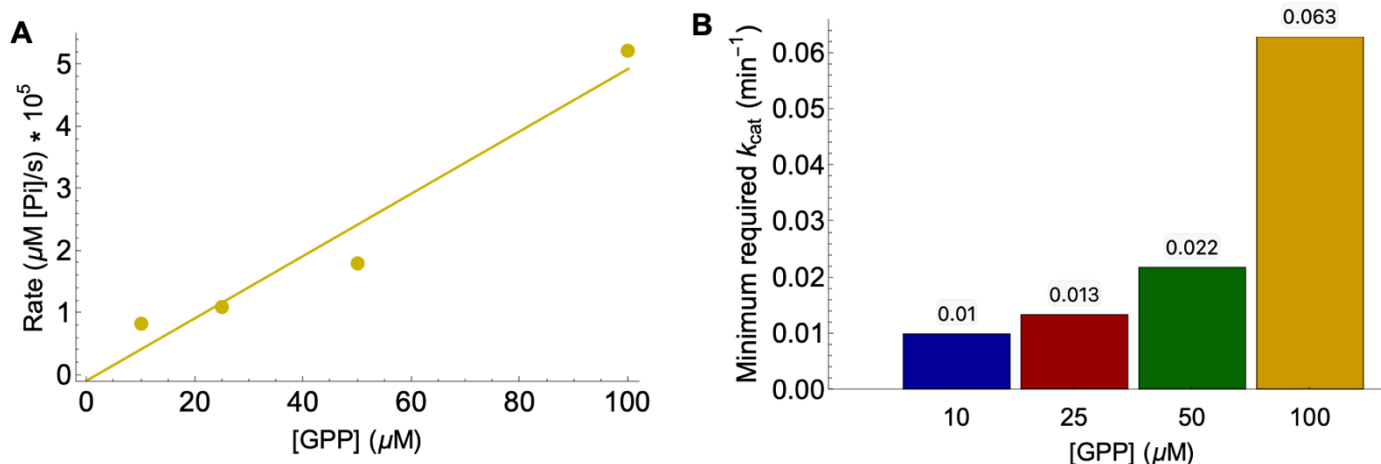


Figure 5. Measurement of the background rate of GPP hydrolysis and implications for assay development. (A) Relationship between GPP concentration and rate of uncatalysed GPP hydrolysis (B) Minimum k_{cat} values for the TS to measure its kinetics at each GPP concentration. The minimum k_{cats} were obtained using the following formula: $k_{\text{cat}} = V_{\text{max}} / 0.05 \mu\text{M}$ (where 0.05 μM is the maximum enzyme concentration possible in future on-chip HT-MEK assays).

Ensuring PPase does not hydrolyse GPP and PPI hydrolysis is not rate-limiting

Although enzymes have maximum activity towards their cognate substrates, many have “promiscuous” activities (4). In the previous section we assumed that the production of P_i was due to uncatalysed hydrolysis, but an alternative model was that PPase might promiscuously hydrolyse GPP. To test this, we measured the rate of P_i production at two PPase concentrations and two GPP concentrations (Fig. 6). Uncatalysed GPP hydrolysis predicts that the observed rate will be invariant with respect to $[PPase]$, while PPase catalysis predicts rates linearly proportional to $[PPase]$. Although the rates were modestly higher at higher $[PPase]$, we did not observe the expected 5-fold increase, indicating negligible activity for GPP, although further experiments are necessary. Similarly, additional experiments are needed to confirm PP_i hydrolysis is not rate-limiting, although the increase in rate for 100 vs. 50 μM GPP hydrolysis is consistent with this.

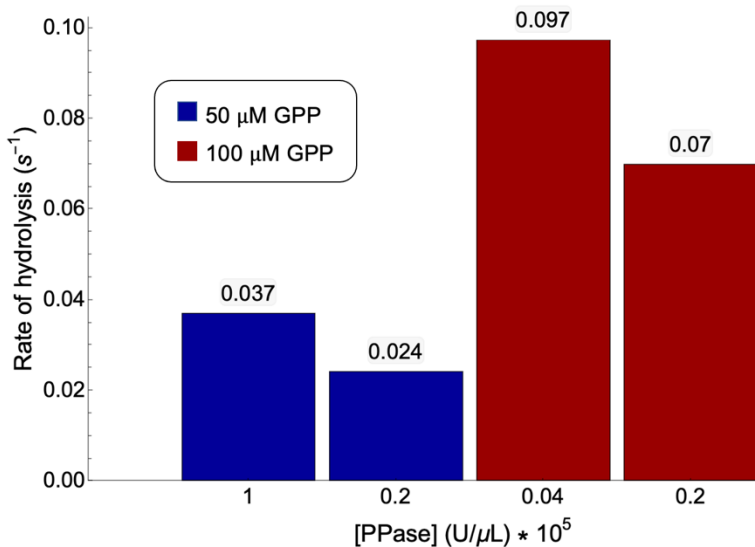
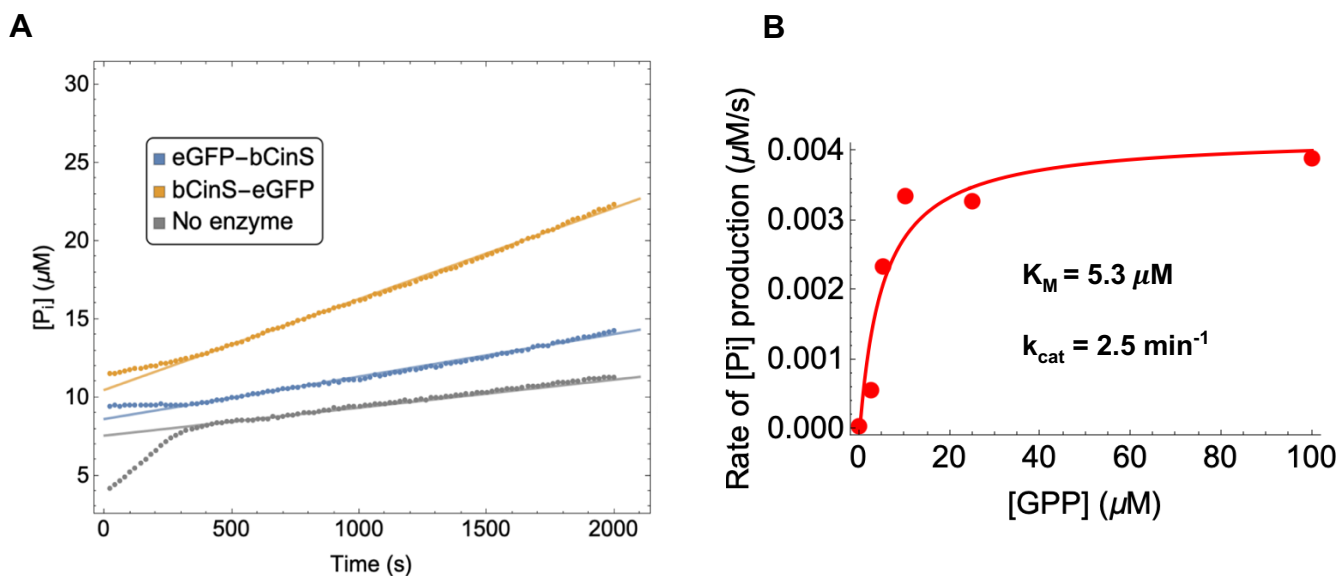


Figure 6. PPase rate of hydrolysis at 50 μM (blue) and 100 μM (red) with varying PPase dilutions. The rates of hydrolysis were obtained via initial rate fits from reaction progress curves. The diluted PPase concentrations in U/ μL were calculated by dividing the stock concentration (0.1 U/ μL) by the dilution.

Measuring bCinS kinetics and comparing effect of traditional *E. coli*-based and cell-free expression

We asked whether we could use our assay to measure the kinetics of bCinS expressed in *E. coli*, a well-characterized TS whose product is cineole (5). We measured initial rates of P_i production at $[GPP]$ ranging from 0 μM to 100 μM and fit these to the Michaelis-Menten model (Fig. 7b). Parameters agreed with previous measurements in the Scrutton lab (manuscript in preparation).

The HT-MEK technology relies on cell-free expression to produce enzymes *in situ* and an eGFP tag for purification. As a step towards developing the high-throughput assay, we expressed bCinS with N and C-terminal eGFP tags in the PURExpress system and used our assay to measure activity under k_{cat} conditions. The N-terminal eGFP tag appears to compromise activity, while C-terminal tagging is well tolerated, based on k_{cat} values matching *E. coli*-expressed and untagged bCinS (Fig. 7c).



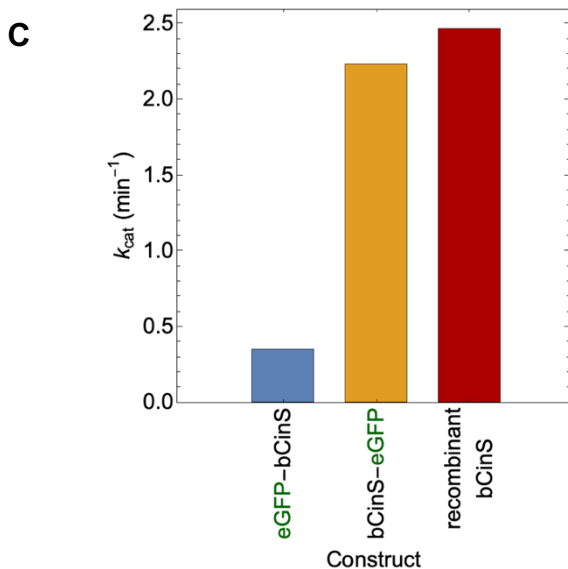


Figure 7. Measurement of the TS bCinS kinetics using our coupled fluorogenic assay. (A) Progress curves of P_i production by different bCinS constructs and a no enzyme control. (B) Michaelis-Menten curve of recombinant bCinS (C) Comparison of k_{cat} values calculated for different bCinS constructs.

Discussion

The feasibility of our coupled assay was validated by our ability to measure rates of bCinS. More replicates and controls will have to be performed in certain cases. An issue was trace P_i in buffers and substrate stocks. We took steps to ensure experiments were not hindered by this; however, we will have to implement further strategies to minimise P_i contamination. The data also serves as foundation for modelling the coupled assay system for further optimisation. Incorporation of our assay into HT-MEK is another next step.

Our project and the Biochemical Society

This project represents much of what Biochemical Society aims to achieve and uphold. I gained experience in biochemistry (assay design, kinetics, cell-free protein expression) as well as bioinformatics and engineering. Collaborating with Dr Faulkner, we are developing a method to identify putative terpene synthases from sequence databases. With Dr Markin, I helped engineer a bespoke fluorescence imager (Fig. 8). Furthermore, our data supported a successful grant application, advancing the project's future.

This project serves as a foundation for research into high-throughput enzyme characterisation. This goal will further facilitate transition towards a circular bioeconomy, benefiting society both environmentally and economically.

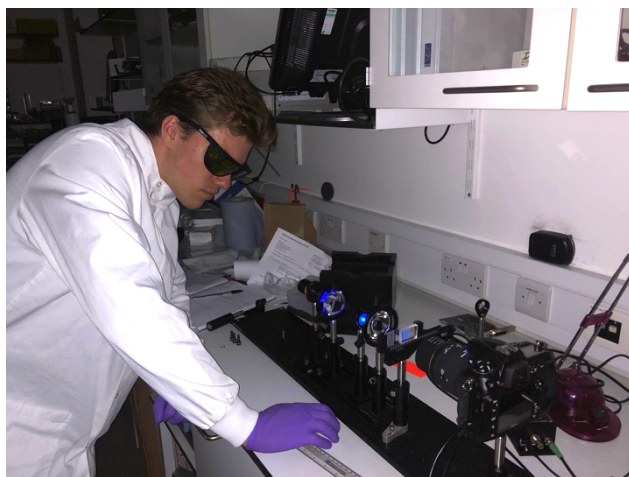


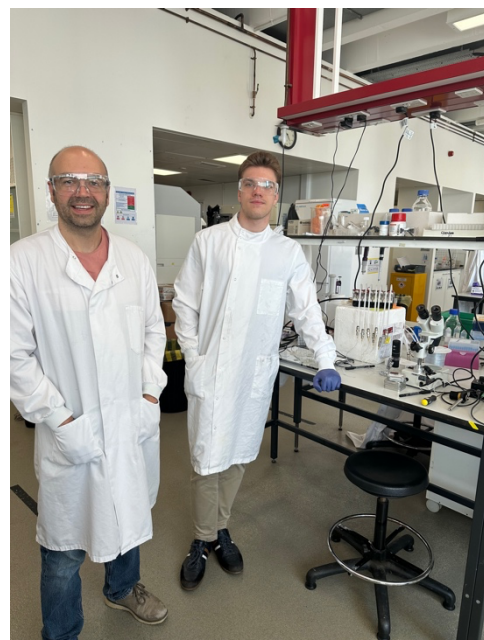
Figure 8. Arseniy working on the bespoke fluorescence imager for measurement of on-chip fluorescence.

Acknowledgements

I would like to sincerely thank the Biochemical Society for providing me with this opportunity to gain hands-on research experience in the area of my academic interest. I am extremely grateful to Dr Craig Markin for supervising me and accommodating me during my 6-week placement at the Manchester Institute of Biotechnology. I am also grateful to Dr Matt Faulkner, Dr Joshua Whitehead and Sahara Bhanot for providing their expertise and assisting in the project.

This studentship has given me a wealth of practical experience which no textbook can ever provide. Over the course of our work, we encountered various challenges and had to discuss and adjust our methodology accordingly. I look forward to continuing working with Dr Markin during my 3rd year and in my 4th year for my Master's.

Figure 9. Dr Craig Markin (left) and Arseniy (middle) standing next to HT-MEK (right).



References

1. Markin CJ, Mokhtari DA, Sunden F, Appel MJ, Akiva E, Longwell SA, et al. Revealing enzyme functional architecture via high-throughput microfluidic enzyme kinetics. *Science*. 2021;373(6553):eabf8761.
2. Markin CJ, Mokhtari DA, Du S, Doukov T, Sunden F, Cook JA, et al. Decoupling of catalysis and transition state analog binding from mutations throughout a phosphatase revealed by high-throughput enzymology. *Proceedings of the National Academy of Sciences*. 2023;120(29):e2219074120.
3. Brune M, Hunter JL, Corrie JE, Webb MR. Direct, real-time measurement of rapid inorganic phosphate release using a novel fluorescent probe and its application to actomyosin subfragment 1 ATPase. *Biochemistry*. 1994;33(27):8262-71.
4. O'Brien PJ, Herschlag D. Catalytic promiscuity and the evolution of new enzymatic activities. *Chemistry & Biology*. 1999;6(4):R91-R105.
5. Karuppiah V, Ranaghan KE, Leferink NGH, Johannissen LO, Shanmugam M, Ní Cheallaigh A, et al. Structural Basis of Catalysis in the Bacterial Monoterpene Synthases Linalool Synthase and 1,8-Cineole Synthase. *ACS Catalysis*. 2017;7(9):6268-82.